# Supplementary Information

## Morphology and composition controlled growth of polar *c*- and nonpolar *m*-axis well-aligned ternary III-nitride nanotube arrays

*Huijie Li,*[*a] *Guijuan Zhao,*[a] *Susu Kong,*[a] *Dongyue han,*[a] *Hongyuan Wei,*[a] *Lianshan Wang,*[a] *Zhen Chen*[b] *and Shaoyan Yang*[*a]

[a]. Key Laboratory of Semiconductor Materials Science and Beijing Key Laboratory of Low Dimensional Semiconductor Materials and Devices, Institute of Semiconductors, Chinese Academy of Sciences, P. O. Box 912, Beijing 100083, People's Republic of China

[b]. LatticePower (Jiangxi) Corporation, No. 699 North Aixihu Road, National High-Tech Industrial Development Zone, Nanchang, Jiangxi 330029, People's Republic of China.

Corresponding author: hjli2009@semi.ac.cn, sh-yyang@semi.ac.cn

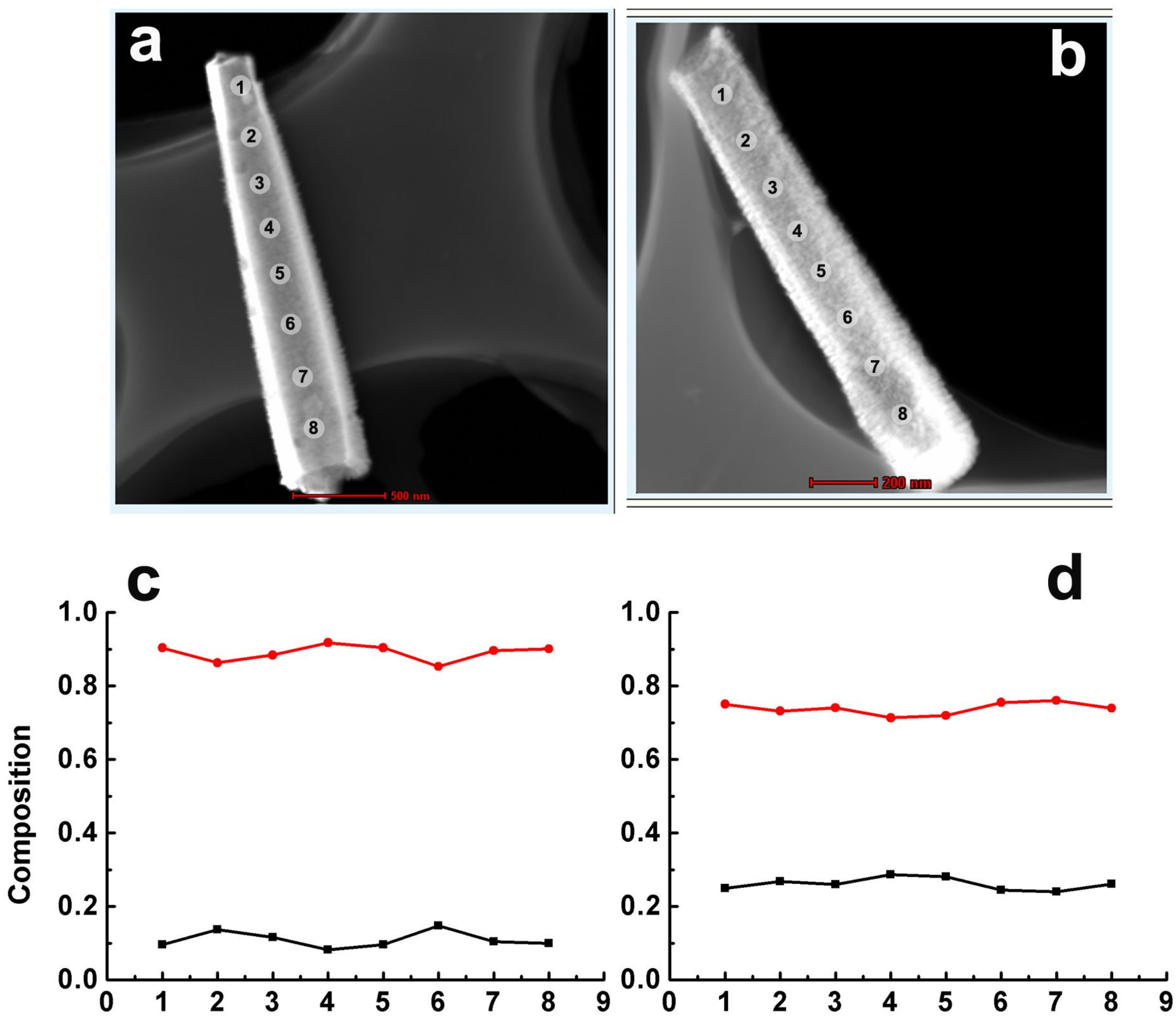


**Figure S1.** Analysis of the In and Al composition along the nanotube growth direction by TEM-EDXS. (a), (c) TEM image and elemental distribution of a low In content (~10%) InAlN nanotube; (b), (d) The elemental distribution analysis of a InAlN nanotube with relatively higher In content (~25%). Both the InAlN nanotubes have relatively homogeneous In composition along the tube axis, no progressive variation of the In content was observed.

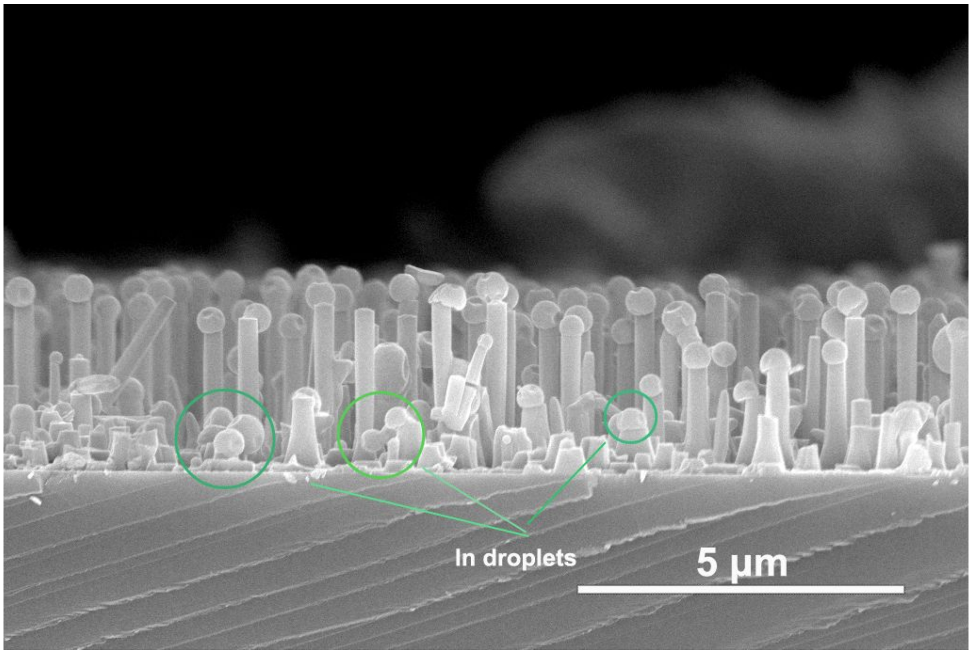


**Figure S2.** Side-view SEM image of the InN nanorods grown on *c*-sapphire. Most of the nanorods have similar length of about 2~3 μm. However, along with the long nanorods, there are some InN nanorods have very short length (marked in green circles). The In droplets on the short nanorods may also contribute to the In incorporation into the InAlN nanotubes.

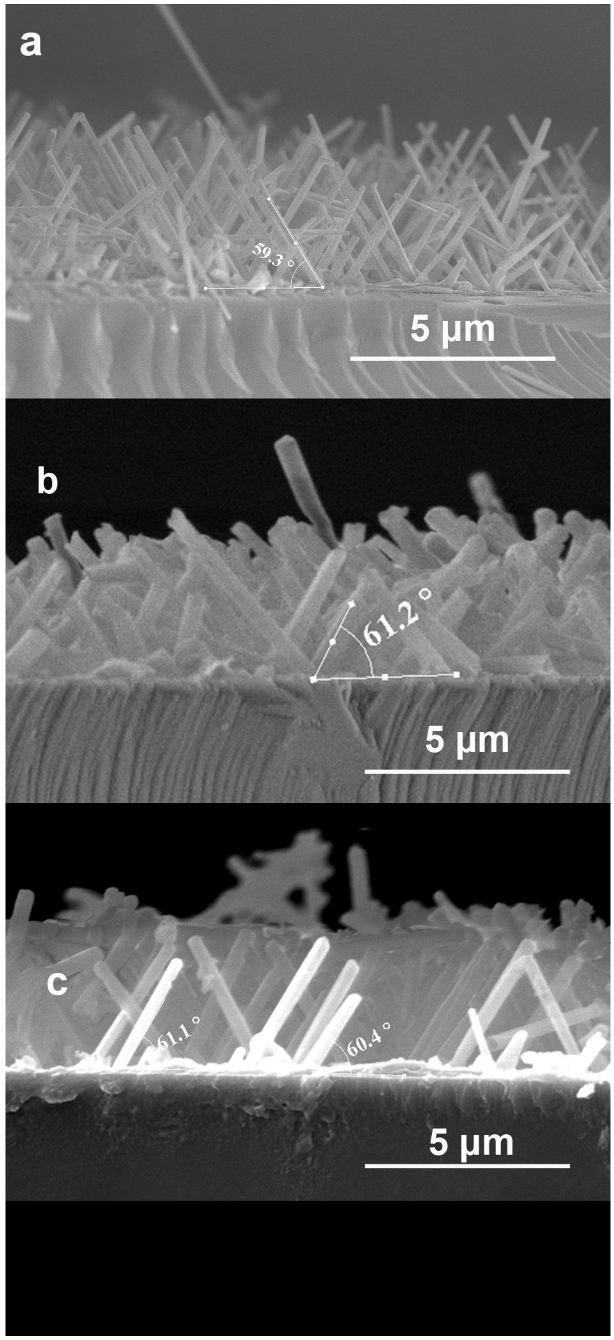


**Figure S3.** Side-view SEM images of nanorods/nanotubes grown on the *r*-plane sapphires. (a) HCl-etched InN nanorods, (b) nanotubes synthesized using the as-synthesized InN nanorods, and (c) nanotubes synthesized using the HCl-etched InN nanorods. The angles between the nanorods/nanotubes and the substrates are about 60°, thus the angles between the nanorods/nanotubes and the substrate normal are about 30°.

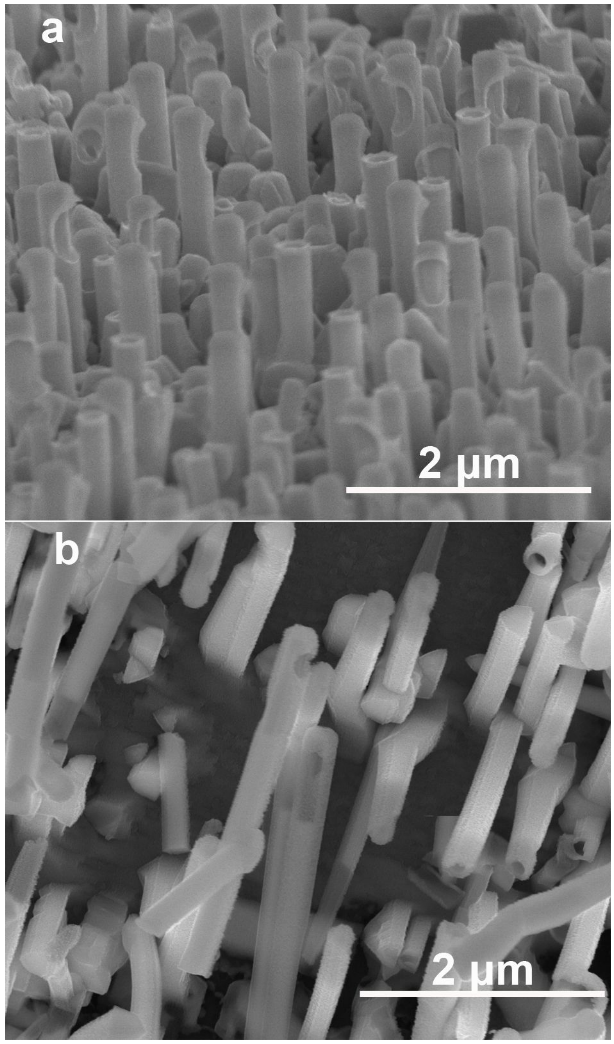


**Figure S4.** After being etched in HCl solution, the In droplets on the sidewalls of the AlN coated InN nanorods formed at 620 °C disappeared and small holes were exposed. (a) and (b) are the representative SEM images of the *c*- and *m*-axis samples, respectively.

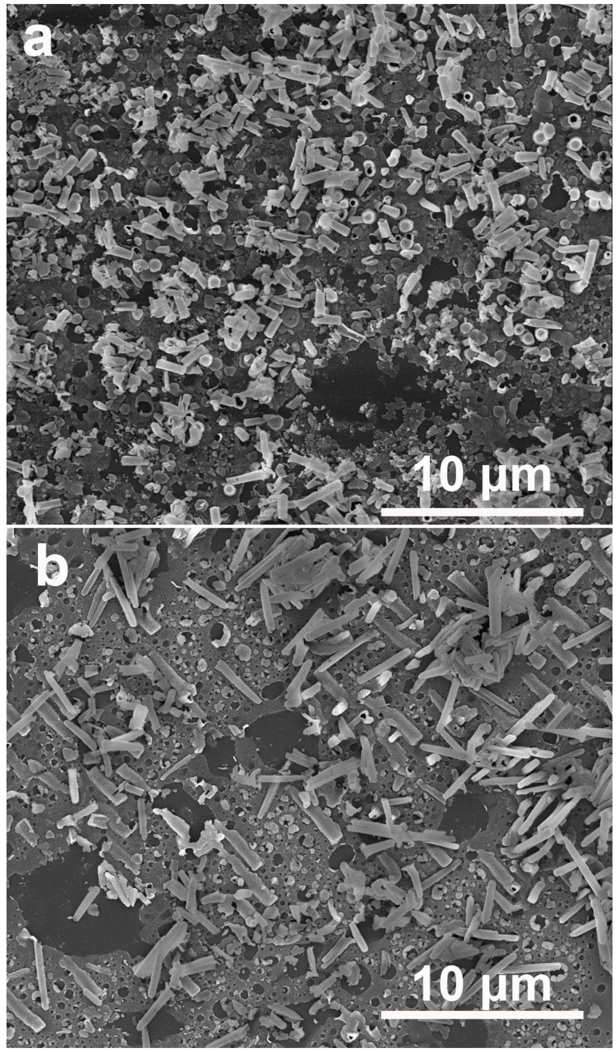


**Figure S5**. SEM images of the nanotubes synthesized by depositing AlN at 670 °C on (a) *c*-axis and (b) *m*-axis InN nanorods. The nanotubes are no more well-aligned on the substrates.

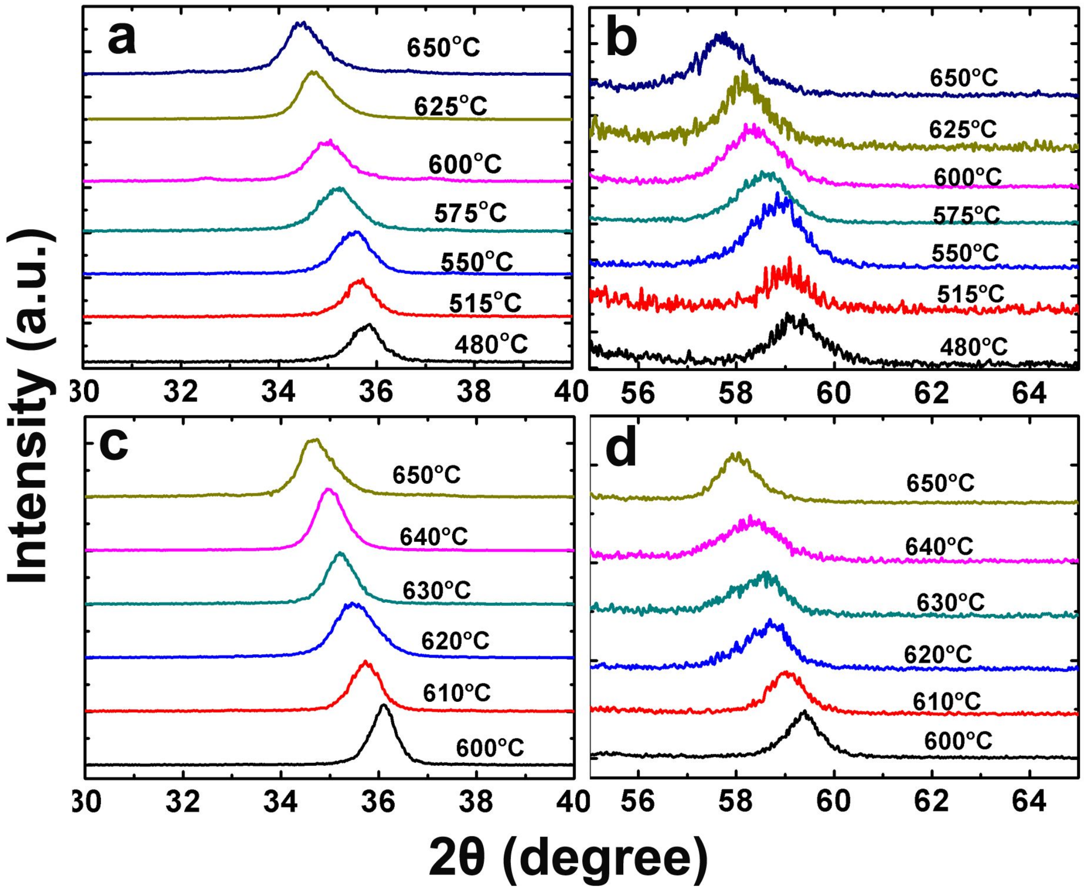


**Figure S6**. XRD patterns of the nanotubes formed at different AlN deposition temperatures. (a) *c*-axis and (b) *m*-axis nanotubes grown using the as-synthesized InN nanorods. (c) *c*-axis and (d) *m*-axis nanotubes grown using the HCl-etched InN nanorods. The XRD peaks of the products progressively shifted toward the lower angle side with the increasing AlN deposition temperature, indicating the In content in the products increases with the temperature.

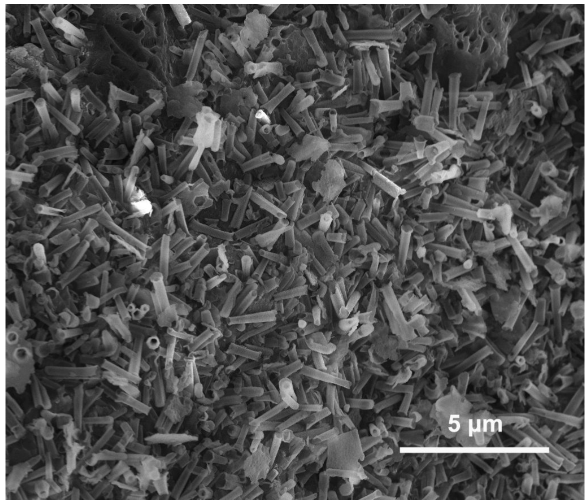


**Figure S7**. SEM images of the InAlN nanotubes after being transferred to the Cu substrate. The transference was realized by pressing the conductive carbon tapes on the sample surface. Then the carbon tapes were pulled apart from the sample and pasted to the Cu foils.

**Table S1**. Comparison of the In contents obtained by XRD and EDAX of the InAlN nanotube samples fabricated at 575~650 °C.

| | Temperature (°C) | In composition obtained by XRD | In composition obtained by EDAX |
|---|---|---|---|
| *c*-axis InAlN nanotubes | 575 | 0.145 | 0.13 |
| | 600 | 0.173 | 0.15 |
| | 625 | 0.24 | 0.23 |
| | 650 | 0.29 | 0.25 |
| *m*-axis InAlN nanotubes | 575 | 0.09 | 0.07 |
| | 600 | 0.12 | 0.13 |
| | 625 | 0.16 | 0.16 |
| | 650 | 0.19 | 0.17 |

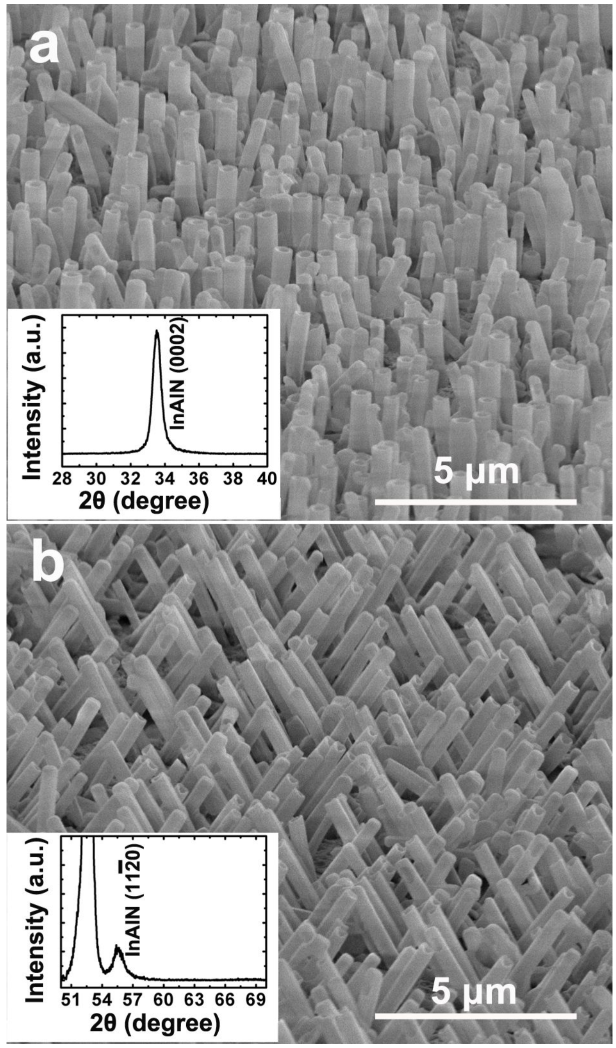


**Figure S8**. High In content InAlN nanotubes synthesized by introducing TMIn into the chamber when depositing AlN epilayers. The TMIn/TMAl flow ratio was set to 1:1. (a), (b) SEM images of the nanotubes grown on *c*- and *r*-plane sapphire substrates, respectively. Insets in (a) and (b) are the corresponding XRD patterns of the products. The peak positions of the products in (a) and (b) are 33.32° and 55.58°, respectively. The In compositions are calculated by the Vegard's rule (Eq. (1)) to be 0.54 and 0.45 for the *c*- and *m*-axis nanotubes, respectively.